Acta Biomaterialia 16 (2015) 178–186

Contents lists available at ScienceDirect

Acta Biomaterialia

journal homepage: www.elsevier.com/locate/actabiomat

Asymmetric flexural behavior from bamboo's functionally graded hierarchical structure: Underlying mechanisms

Meisam K. Habibi [a], Arash T. Samaei [a], Behnam Gheshlaghi [a], Jian Lu [a,b], Yang Lu [a,b,*]

[a] Department of Mechanical and Biomedical Engineering, City University of Hong Kong, 83 Tat Chee Avenue, Kowloon, Hong Kong, China
[b] Centre for Advanced Structural Materials (CASM), City University of Hong Kong, 83 Tat Chee Avenue, Kowloon, Hong Kong, China

ARTICLE INFO

Article history:
Received 15 August 2014
Received in revised form 18 December 2014
Accepted 27 January 2015
Available online 4 February 2015

Keywords:
Bamboo
Flexural behavior
Functionally graded structure
Asymmetry
Bio-inspired structural materials

ABSTRACT

As one of the most renewable resources on Earth, bamboo has recently attracted increasing interest for its promising applications in sustainable structural purposes. Its superior mechanical properties arising from the unique functionally-graded (FG) hierarchical structure also make bamboo an excellent candidate for bio-mimicking purposes in advanced material design. However, despite its well-documented, impressive mechanical characteristics, the intriguing asymmetry in flexural behavior of bamboo, alongside its underlying mechanisms, has not yet been fully understood. Here, we used multi-scale mechanical characterizations assisted with advanced environmental scanning electron microscopy (ESEM) to investigate the asymmetric flexural responses of natural bamboo (*Phyllostachys edulis*) strips under different loading configurations, during "elastic bending" and "fracture failure" stages, with their respective deformation mechanisms at microstructural level. Results showed that the gradient distribution of the vascular bundles along the thickness direction is mainly responsible for the exhibited asymmetry, whereas the hierarchical fiber/parenchyma cellular structure plays a critical role in alternating the dominant factors for determining the distinctly different failure mechanisms. A numerical model has been likewise adopted to validate the effective flexural moduli of bamboo strips as a function of their FG parameters, while additional experiments on uniaxial loading of bamboo specimens were performed to assess the tension–compression asymmetry, for further understanding of the microstructure evolution of bamboo's outer and innermost layers under different bending states. This work could provide insights to help the processing of novel bamboo-based composites and enable the bio-inspired design of advanced structural materials with desired flexural behavior.

1. Introduction

Biological materials, such as plants and animal bones, tend to be optimized for the loading conditions they are subjected to. They are not only promising for engineering applications owing to their availability and mechanical performance [1], but also are excellent candidates for the mimicking purposes to design new bio-inspired materials for structural purposes [2,3]. Among biological materials, bamboo is one of the most proficient candidates owing to its superior mechanical properties and unique hierarchical structure. Bamboo culms are essentially optimized unidirectional fiber-reinforced composites with cellular parenchyma as the matrix (see Fig. 1). They also perfectly demonstrate the concept of functionally graded materials (FGMs) in which continuously graded properties are specified by spatially varying microstructure stemmed out from non-uniform distribution of different constituents [4,5]. By having smooth variation in properties, FGMs may offer advantages such as reduction of stress concentration and increased bonding strength [4,6].

With the notion of mimicking natural structures for synthesis of new structural materials, the quest to understand the relationship between bamboo's hierarchical graded structure and its mechanical behavior (particularly its impressive flexibility) has recently attracted considerable attentions [7–13]. In an attempt, Obataya et al. [8] demonstrated that the bamboo culm is flexible when its stiff outer layer is strained while softer inner layer is compressed. Basically, they attributed the excellent flexural ductility of split bamboo culm to the combination of fiber rich outer parts and compressible inner parts. In a different study, Tan et al. [11] showed that, in the course of bending deformation on a single edge notched specimen, the crack growth occurs by deflection into interlaminar

* Corresponding author at: Department of Mechanical and Biomedical Engineering, City University of Hong Kong, 83 Tat Chee Avenue, Kowloon, Hong Kong, China. Tel.: +852 3442 4061.
E-mail address: yanglu@cityu.edu.hk (Y. Lu).

http://dx.doi.org/10.1016/j.actbio.2015.01.038
1742-7061/

boundaries. Low et al. [5] also demonstrated that the excellent damage tolerance of bamboo can be mainly attributed to the interplay and concurrent display of crack-deflection, fiber-debonding and crack bridging as the major energy dissipative processes.

In light of the earlier studies, it appears that the asymmetric flexural behavior of bamboo strips along with its underlying deformation mechanisms at the microstructural level has not yet been fully explored, despite a very recent research dealing with bamboo material's anisotropic gradient mechanical behavior [2]. Even, among those limited efforts on bending characterization of bamboo strips, it appears that investigations pertaining to the FG structure of bamboo have been paid great attention to [2,8], whereas the important fracture behavior, alongside their corresponding failure mechanisms interacted with the hierarchical structure of bamboo, has been often underrated [14]. Likewise, to facilitate the implementation of experimental results for bio-mimicking purposes, there is a need for developing a proper numerical model to predict the gradient flexural behavior of bamboo strips along their thicknesses with full consideration of their hierarchical biological structures. Together with the inputs from the experimental studies, such a model could be also used for further development of FG-structure induced asymmetry for desired structural purposes.

2. Samples and experimental procedures

The Moso or "Mao Zhu" bamboos (belonging to *Phyllostachys edulis* species), collected from bamboo plantations located in Jiangsu and Zhejiang provinces in China were selected as the raw materials for this study. They were all mature bamboo (~5 years old), cut from the middle section of stalk, and were kept at room temperature of ~23 °C and relative humidity of ~55–70% (close to the humidity level of bamboo's natural habitat ~60–80%).

To evaluate the flexural behavior of bamboo, bamboo strips were prepared along the culm thickness with different fiber volume fractions. As demonstrated in Fig. 2, strips prepared from the outer part (Red: 4×4.2 mm^2) comprised the highest amount of fibers, whereas the fiber volume fraction kept diminishing as the thickness of the strips approached the entire thickness of bamboo culm (Blue: 6×6.2 mm^2 and Green: 8×8.2 mm^2). The bamboo strips, with ambient humidity level, were subsequently subjected to Three-Point (3-P) bending by using Tinius Olsen 50KT Material Testing System (MTS) with displacement rate of 0.01 mm/s. The ambient humidity (~55–70%) and temperature (~23 °C) level were chosen for the mechanical characterizations to stimulate the actual working condition of bamboo alongside avoiding any drying artifacts. The flexural modulus of each strip was finally extracted from the stress–strain curve through Eq. (1) which is given below [15]:

$$E_f = \frac{L^3 m}{4wd^3} \tag{1}$$

where E_f is the flexural modulus of elasticity, m is the gradient (i.e., slope) of the initial portion of the load–deflection curve, L is the support span, w is the width of the specimen and d is the thickness.

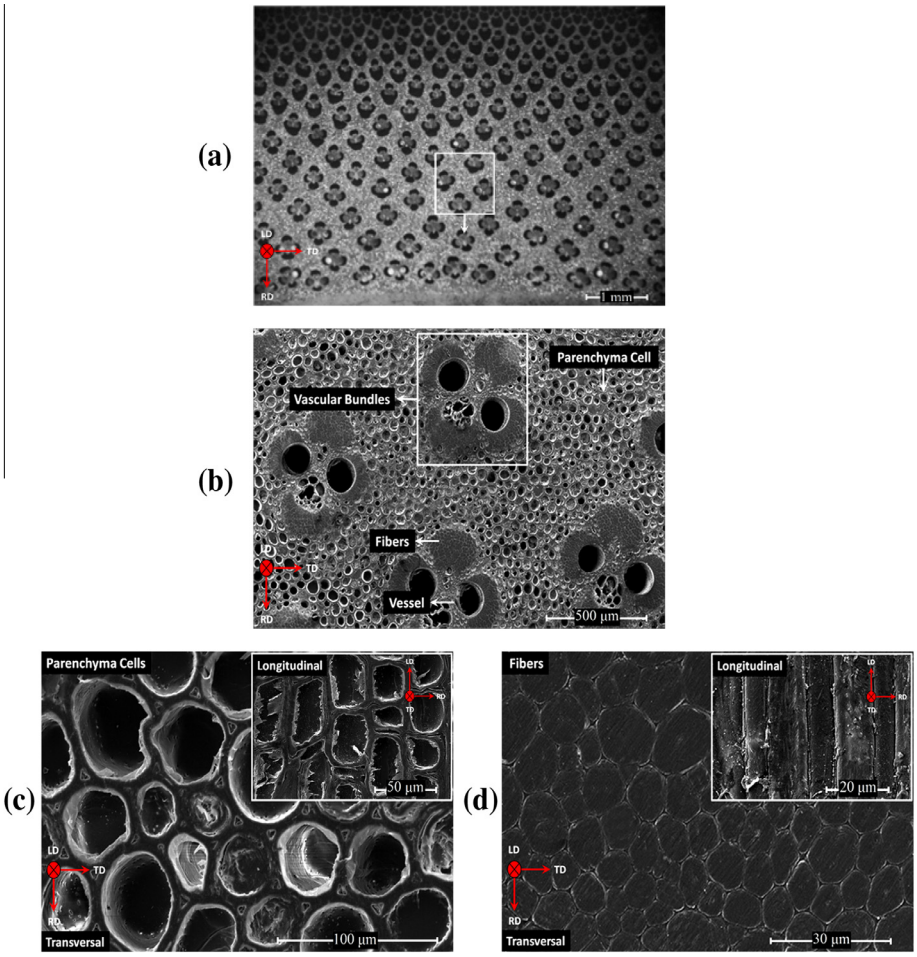

Fig. 1. Functionally graded (FG) hierarchical structure of bamboo: optical and SEM micrographs (a and b) representing the microstructure of bamboo culm with different constituents; (c) parenchyma cells and (d) bamboo fibers (viewed in transverse direction). The insets in (c) and (d) show the microstructure of parenchyma cells and bamboo fibers in longitudinal direction, respectively.

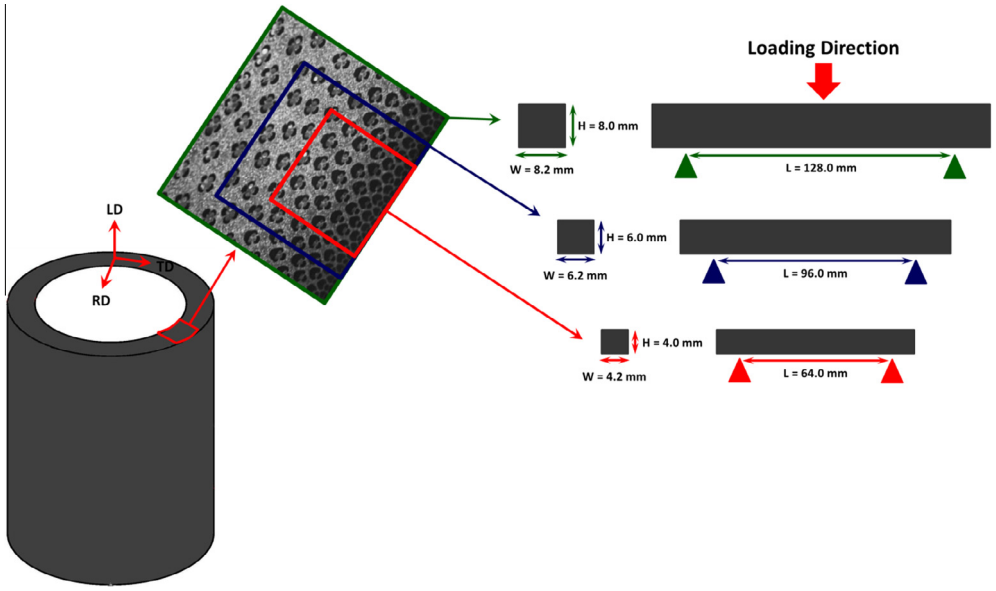

Fig. 2. Samples and experimental configuration: schematic representation of bending samples prepared from longitudinal section of bamboo culm (green refers to whole thickness (~8 mm), whereas blue and red refer to 75% and 50% of the culm thickness, respectively).

To obtain the necessary materials properties data for the numerical analysis, load controlled nano-indentation experiments were conducted [16,17] on bamboo fibers along with parenchyma cells, respectively, to measure their young's moduli. To assure the validity of the results, 50 indentations were conducted, separately, on both fibers and parenchyma cells. A Hysitron TI 750 Ubi™ nano-indenter with a cube corner tip (Radius ~ 100 nm) was employed for this purpose. A maximum force of 700 μN was achieved in the course of 5 s. Following 10 s holding period, the load was then released over 5 s. The reduced moduli (E_r) along with its subsequent young's moduli (E_s), defined as below [18], were finally extracted from the unloading region of load–displacement curves.

$$E_r = \frac{1}{\beta}\frac{\sqrt{\pi}}{2}\frac{1}{\sqrt{A_p}}\frac{dp}{dh} \tag{2}$$

$$\frac{1}{E_r} = \frac{(1-\nu_i^2)}{E_i} + \frac{(1-\nu_s^2)}{E_s} \tag{3}$$

where A_P is the projected contact area, β is a geometrical constant that is 1.034 for a cube corner tip [16], and $\frac{dp}{dh}$ is the initial stiffness at the onset of unloading. In Eq. (3), the subscripts "i" and "s" stand for the indenter and substrate, respectively and ν is the Poisson's ratio. For the diamond indenter tip, the E_i and ν_i are 1140 GPa and 0.07, respectively, whereas the ν for bamboo fibers is found to be 0.22 [19]. In view of lack of experimental data on the Poisson's ratio of bamboo's parenchyma cells, the reported value for the parenchyma cells of other biological species, 0.4, is considered here [20].

The microstructural characterizations were conducted by FEI Quanta 450 FEG Scanning Electron Microscope with ESEM mode, which allows the revelation of bamboo's different constituents as well as its functionally graded hierarchical structure at high resolution, along with an Olympus/SZX12 Stereo Optical Microscope for fracture surface examinations.

3. Results

3.1. Gradient flexural behavior

In view of bamboo strips' hierarchical functionally graded (FG) structure, as displayed in Fig. 1, fibers are densely distributed in the outer part while sparsely dispersed in the inner part, whereas parenchyma cells are densely and sparsely distributed in inner and outer parts, respectively. The exhibited graded distribution of fibers and parenchyma cells naturally aroused a functionally gradient mechanical behavior along the thickness of the strips which is schematically depicted in Figs. 3 and 4 and summarized in Table 1, respectively (Mode A refers to loading on higher fiber density side, whereas Mode B stands for loading on lower fiber density side). Our mechanical characterizations demonstrated that bamboo strips prepared from the outer part (Red color: 4×4.2 mm^2), with high fiber volume fraction, exhibited high flexural moduli and strengths. However, as the thickness of the strips approached the entire thickness of bamboo culm (Blue: 6×6.2 mm^2 and Green: 8×8.2 mm^2), their respective flexural moduli and strengths diminished (see Figs. 3a and 4a–b), which is mainly owing to the reduction in fiber volume fraction (see Table 1).

Similarly, bamboo strips exhibited a graded flexural behavior in terms of their flexibility and flexural toughness, which could be once again attributed mainly to graded distribution of fibers and parenchyma cells along the thickness of the strips. Flexibility, here, was defined as the flexural strain at the fracture point, whereas flexural toughness was considered as the area under the stress–strain curves up to the failure point. Since, bamboo strips exhibited a non-catastrophic fracture with extensive delamination, similar to fiber reinforced polymer composites and laminates [5,21], 40% drop in the loading was considered as the material's failure point, here. As depicted and listed in Fig. 4c–d and Table 1, respectively, strips prepared from near the outer part, with high fiber volume fraction, exhibited considerably large flexibility and toughness. However, as the thickness of the strips approached the entire thickness of bamboo culm, their respective flexibility and flexural toughness diminished.

3.2. Asymmetric flexural behavior

In addition to the exhibited gradient flexural behavior due to the FG distribution of fibers and parenchyma cells along the thickness of the strips, more interestingly, the flexural behavior of bamboo strips also changed as the bending configuration changed. As demonstrated and listed in Figs. 3 and 4 and Table 1, respectively, bamboo strips exhibited relatively larger flexural modulus and strength in the case of Mode A bending configuration compared

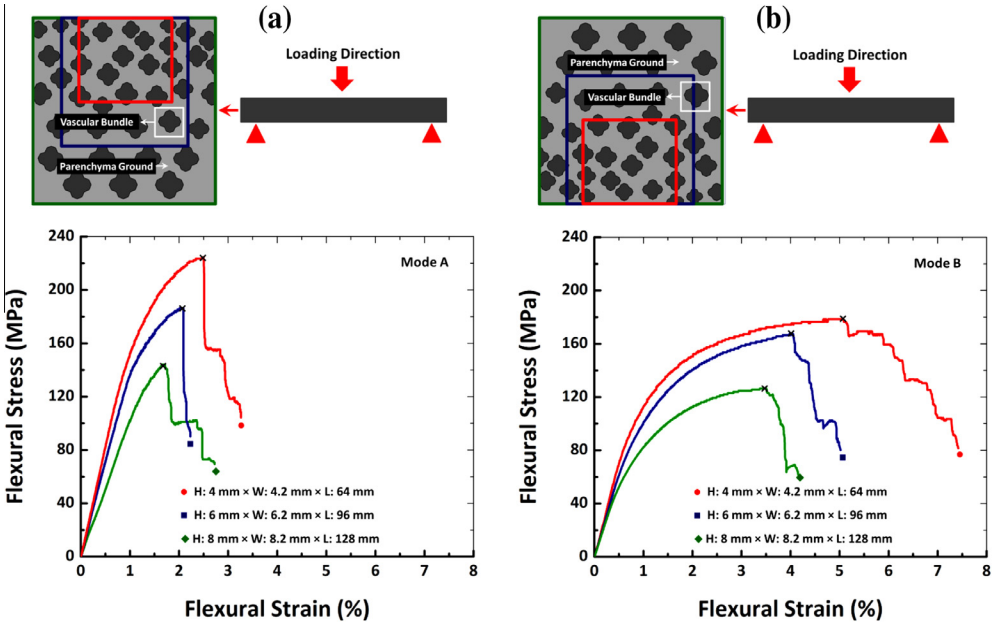

Fig. 3. Selective three-point bending stress–strain curves of bamboo strips, prepared along the culm thickness, in the case of: (a) Mode A (loading on higher fiber density side) and (b) Mode B (loading on lower fiber density side) bending configurations. The cross symbols (×) represent the fracture points, whereas the red circles, blue cubes, and green diamonds stand for bamboo strips failure points (namely, the point where the loading drops down to 40%).

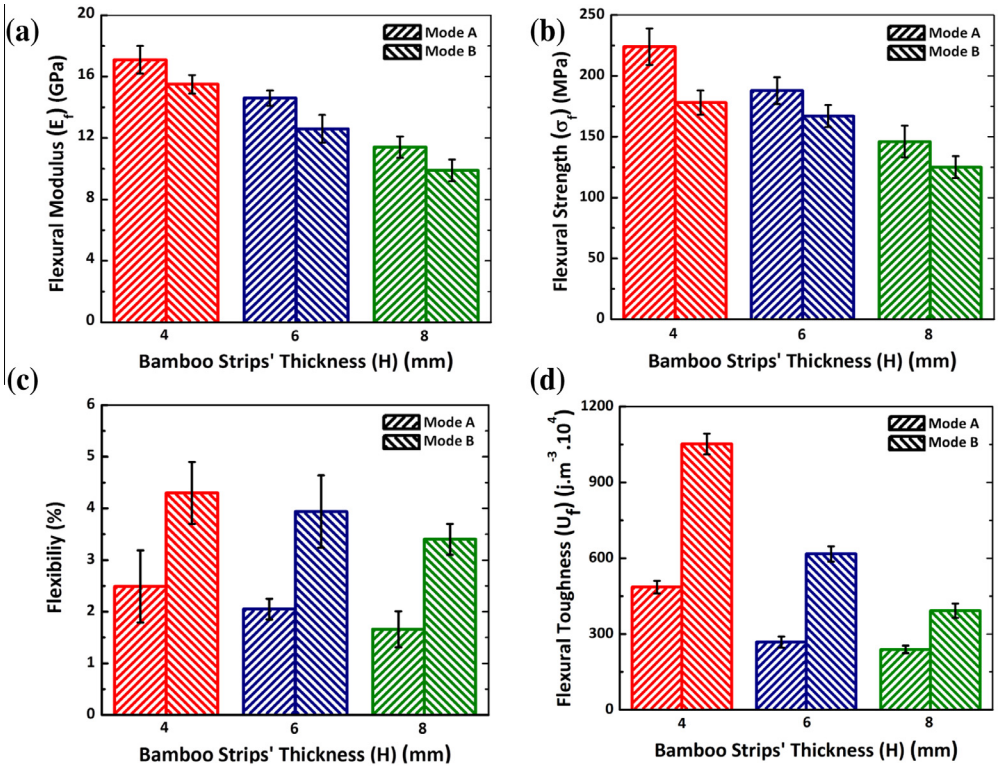

Fig. 4. Asymmetric flexural properties of bamboo strips under Mode A and Mode B bending configurations: (a) flexural modulus; (b) flexural strength; (c) flexibility and (d) flexural toughness as a function of strips' thickness.

to Mode B. On the contrary, they demonstrated much larger flexibility and flexural toughness in the case of Mode B compared to Mode A.

The demonstrated asymmetry in flexural behavior of bamboo strips can be further evidenced by comparing the shape of the stress–strain curves from their respective loading modes. The stress–strain curves were thus compared in terms of two distinct regimes, namely "elastic bending" and "fracture failure" stages (i.e., before and after fracture point), which are distinguished by the cross marks in Fig. 3. As displayed, in the course of Mode A flexural loading (see Fig. 3a), bamboo strips exhibited a relatively narrow linear region up to the fracture point, whereas they demonstrated a wider linear regime followed by a non-linear region in the course of Mode B. Also, stress–strain curves showed

Table 1
Flexural properties of bamboo strips subjected to different bending modes.

Bamboo Strips	Mode	Flexural Modulus (E_f) (GPa)	Flexural Strength (σ_f) (MPa)	Flexibility (%)	Flexural Toughness (U_f) (J. $m^{-3} \times 10^4$)
Red: 4×4.2 mm^2	A	17.1 ± 0.9	224 ± 15	2.49 ± 0.71	486 ± 25
	B	15.5 ± 0.6	178 ± 10	4.30 ± 0.62	1052 ± 41
Blue: 6×6.2 mm^2	A	14.6 ± 0.5	188 ± 11	2.05 ± 0.24	268 ± 22
	B	12.6 ± 0.9	167 ± 09	3.94 ± 0.51	617 ± 30
Green: 8×8.2 mm^2	A	11.4 ± 0.7	146 ± 13	1.66 ± 0.35	239 ± 15
	B	9.9 ± 0.8	125 ± 09	3.42 ± 0.32	392 ± 28

"Green" refers to whole thickness (~ 8mm), whereas "blue" and "red" refers to 75% and 50% of the culm thickness. Mode A refers to "loading on higher fiber density side", whereas Mode B stands for "loading on lower fiber density side".

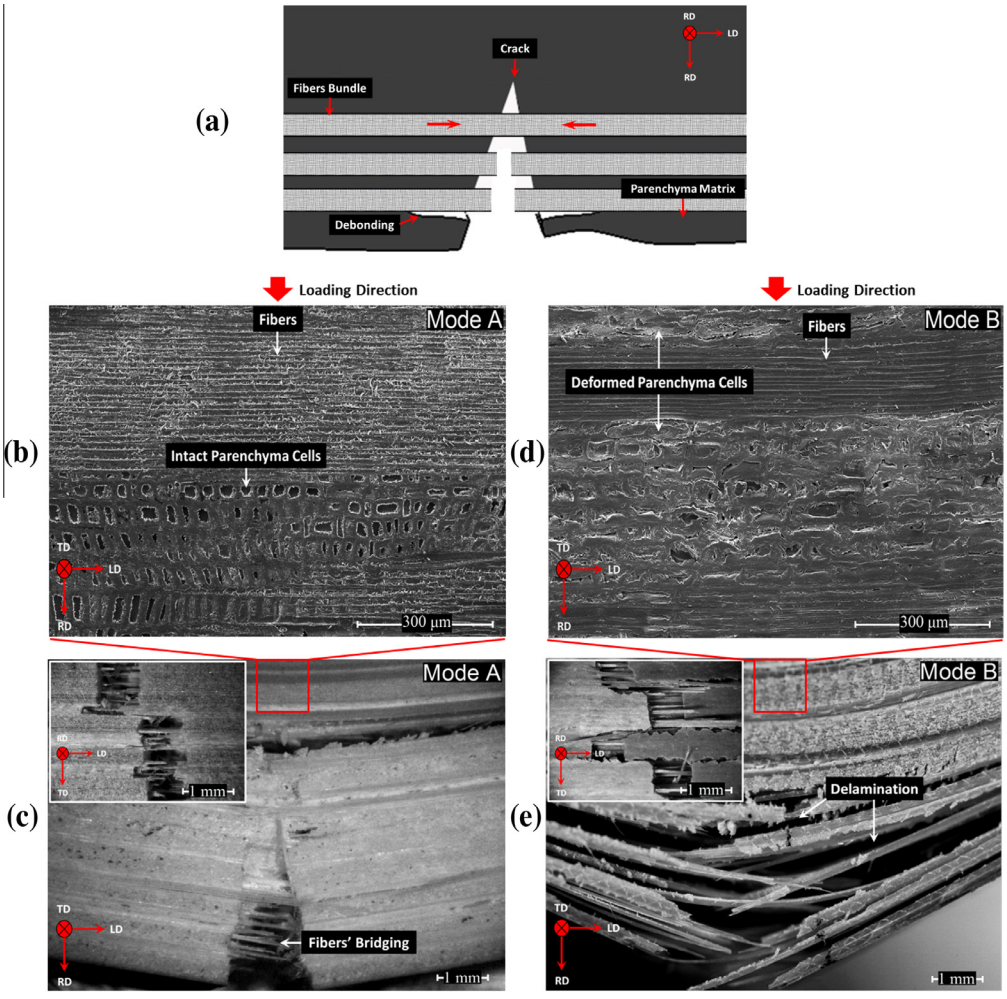

Fig. 5. Fracture mechanisms in different bending configurations: (a) schematic representation of fiber bridging and debonding (red arrows represent the bridging traction acts to restrain the crack opening); for Mode A bending configuration (b and c), optical micrograph (c) shows the fibers bridging in the fractured samples, while (b) displays the compressively deformed areas in the top layer; for Mode B bending configuration (d and e), optical micrograph (e) shows the delamination in the fractured samples, while (d) reveals the deformed parenchyma cells in the top layer. (The insets in (c) and (e) show the extent of fiber bridging and delamination from the bottom surface view, respectively).

less serration in the case of Mode A compared to Mode B. Here, the serrations in the stress–strain curves stand for the occurrence of delamination or debonding of the fiber bundles. Therefore, the different extent of serrations in the case of each loading mode could reveal part of the underlying mechanisms, which might be responsible for the asymmetric flexural behavior of bamboo strips.

4. Discussions

4.1. Mechanisms and modeling of the gradient flexural behavior

The exhibited gradient behavior, especially the flexural modulus and strength of bamboo strips, as listed in Fig. 4a–b and Table 1,

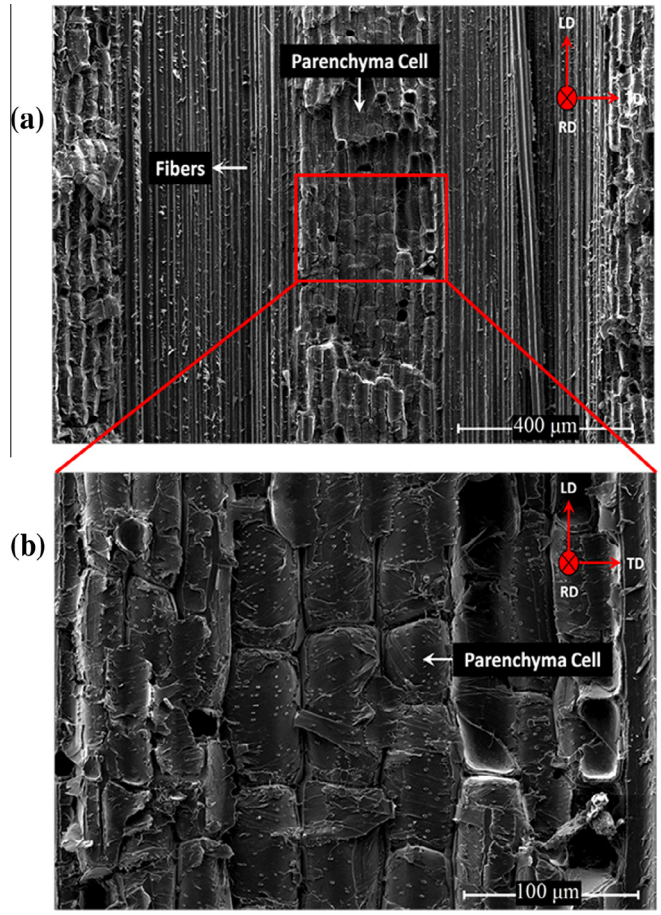

Fig. 6. Occurrence of interfacial fractures within the bamboo fibers and parenchyma cells: (a) in the delaminated areas of a fractured sample; (b) shows the higher magnification view of the wall structure of the intact parenchyma cells.

could be mainly attributed to the graded distribution of vascular bundles, mainly bamboo fibers, along the thickness of the strips. It is already demonstrated that, compared to parenchyma cells (elastic modulus $E_p = 3.7 \pm 0.4$ GPa) [23], fibers are significantly stronger (elastic modulus $E_f = 22.8 \pm 2.8$ GPa) [14,23] and any variation in their volume fraction can affect the overall strength and modulus of bamboo strips, accordingly. The triggered toughening mechanisms such as fibers' bridging (schematically depicted in Fig. 5a) and crack deflection (or so called "tortuous crack propagation") [14] are also partly responsible for the gradient and remarkable flexural strength and toughness of bamboo strips. Hence, as the overall volume fraction of fiber decreased (thickness of the strips approached the entire thickness of bamboo culm), the contribution of triggered toughening mechanisms, due to the presence of fibers, also diminished which resulted in minimizing the flexural strength and toughness of bamboo strips.

In light of the exhibited graded flexural behavior along the thickness of the bamboo strips, a numerical model, capable of predicting the flexural behavior during the elastic bending stage, was primarily introduced here, which could be useful for the implementation of graded structure induced asymmetry from the (bamboo) strips level to bamboo culm level. In this regard, the experimentally derived flexural moduli (see Fig. 4a) were fit into a mathematical method by treating bamboo strip as a FG beam. The necessary material properties were also measured by conducting nano-indentation on bamboo fibers as well as parenchyma cells, individually, to provide estimation for innermost and outermost flexural moduli of bamboo strip, respectively, which were found to be $E_f = 22.8 \pm 2.8$ and $E_p = 3.1 \pm 0.4$ GPa for fibers and parenchyma cells, respectively.

As far as a functionally graded beam with specified width of w, thickness of h and length of L is concerned (see Fig. 7a), the variation of flexural modulus along the thickness can be expressed by the exponential law introduced by Wakashima et al. [25] as below:

$$E(z) = (E_i - E_o)\left(\frac{z}{h} + \frac{1}{2}\right)^k + E_o \tag{4}$$

where E_i and E_o are the flexural modulus at the innermost and outermost layers of bamboo strips, respectively; and k is a FG exponent varying with volume fraction of fiber along the thickness of the strips. Here, we introduced the expression representing the equivalent bending rigidity of bamboo in static equilibrium as following:

$$\begin{aligned} &\int_{-\frac{h}{2}}^{\frac{h}{2}} E(z) w z^2\, dz = \frac{P x^3}{12} + C_1 x + C_2 \qquad 0 \le x \le \frac{1}{2} \\ &\int_{-\frac{h}{2}}^{\frac{h}{2}} E(z) w z^2\, dz = -\frac{P x^3}{12} + \frac{P L x^3}{4} + C_3 x + C_4 \qquad \frac{L}{2} \le x \le L \end{aligned} \tag{5}$$

where $C_1 = -\frac{PL^2}{16}$, $C_2 = 0$, $C_3 = -\frac{3}{4}PL^2$, $C_4 = \frac{PL^3}{48}$ and P is the external static loading.

By using Eqs. (4) and (5) via an iterative manner as well as fitting Eq. (5) to the average value of flexural modulus derived for the largest bamboo strip (8×8.2 mm^2), the parameters in the theoretical model (i.e., E_i, E_0 and k) were measured to be $E_i = 2.78$ GPa, $E_0 = 15.21$ GPa, and $k = 0.43$. The finally introduced model, schematically depicted in Fig. 7b, predicted flexural moduli close to the experimentally derived values for other cross sections (6×6.2 mm^2 and 4×4.2 mm^2). So, in view of the demonstrated close compatibility between the experimentally achieved values (during elastic bending) and their numerically derived counterparts (see Fig. 7b–c), the validity and capability of the introduced numerical model could be verified. This numerical model could also demonstrate how the flexural moduli distribution should be optimized along the thickness in a functionally graded composite structure in order to reach an overall flexural behavior similar to or even better than that of bamboo strip.

4.2. Mechanisms of the asymmetric flexural behavior

4.2.1. Asymmetry during "elastic bending"

Firstly, under different bending configurations, bamboo strips demonstrated a significant asymmetric behavior during the "elastic bending" stage, i.e., before fracture occurred, showing different modulus and flexibility. As displayed in Figs. 4a–c and listed in Table 1, bamboo strips demonstrated larger flexural modulus in the course of Mode A compared to Mode B, which could be easily understood that more fibers were elastically strained while fibers were the major constituent to take load (compared to parenchyma ground). On the contrary, they demonstrated an even larger difference in the flexibility for Mode B compared to Mode A, which could be explained by the fact that more parenchyma cells allow to accommodate much larger deformation by getting squeezed in the compressively deformed areas of the strips in the top layer of Mode B than that of Mode A (see Fig. 5d) while fibers are apparently less elastic deformable. This could be also inferred by a comparison among the shape of the stress–strain curves in the case of each loading mode. Compared to Mode A, stress–strain curves in the case of Mode B (see Fig. 3) exhibited a non-linear deformation regime before the fracture point (see Fig. 3b), which was believed to be associated with the squeezing of parenchyma cells in the course of flexural loading (that is why we called this stage before fracture as "elastic bending" rather than simply "elastic" stage). Lastly, it might be noted that the higher content of parenchyma

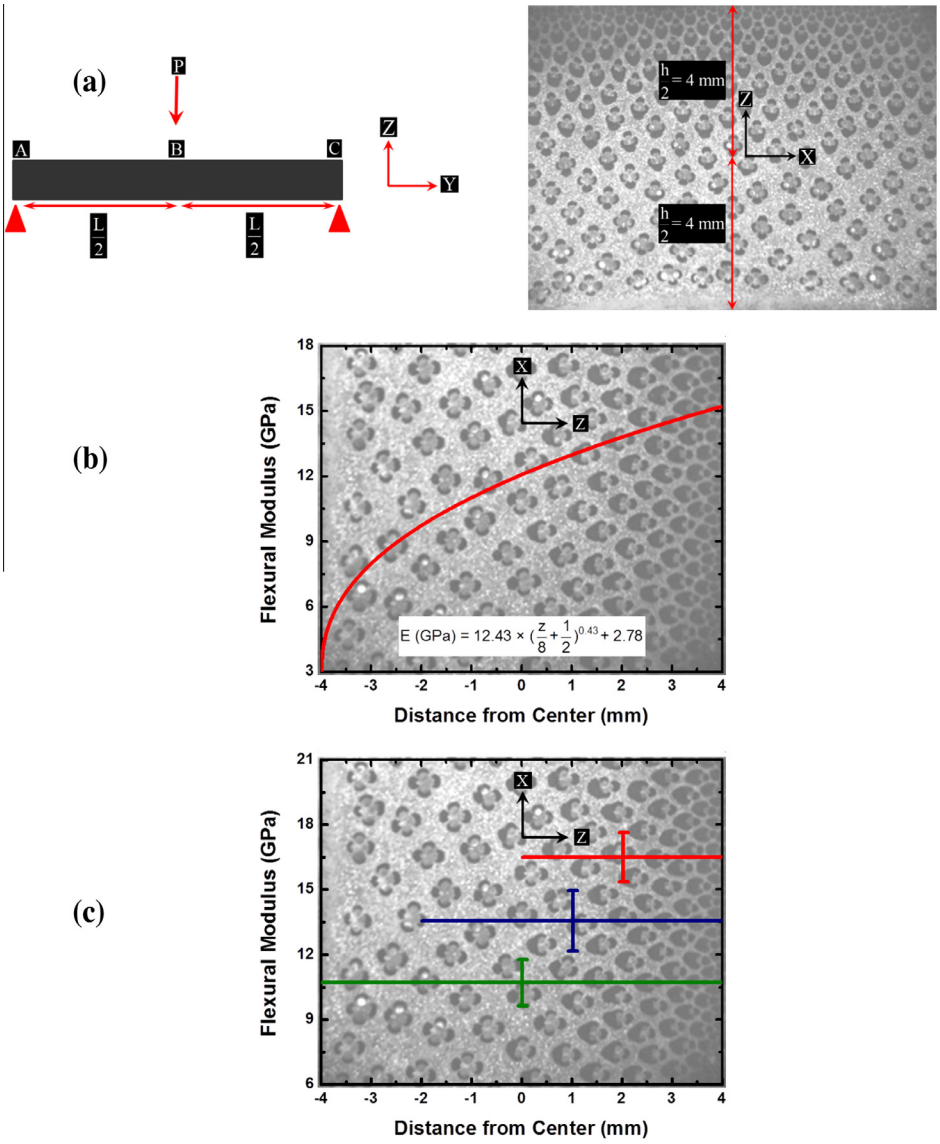

Fig. 7. Distribution of flexural moduli along the bamboo strip thickness: (a) schematic representation of a functionally graded beam used to develop the numerical model along with distribution of flexural moduli along the bamboo strip thickness derived from (b) the introduced numerical model and (c) the experimental characterizations.

cells in the bottom layer in the case of Mode A also increases the strain heterogeneity and the possibility of crack initiation (as fracture always occurred at the bottom side, as shown in Fig. 5c) and subsequent catastrophic failure than that of Mode B, resulted in further lower flexibility.

4.2.2. Asymmetry during "fracture failure"

Furthermore, bent bamboo strips also demonstrated significant asymmetric behavior in the course of "fracture failure", i.e., during and after fracture occurred, displaying different strength and toughness. However, the associated underlying mechanisms here are very different, and more complicated compared to the asymmetry during "elastic bending" stage. As displayed and listed in Fig. 4b–d and Table 1, respectively, bamboo strips exhibited relatively larger flexural strength and much smaller toughness, respectively, in the course of Mode A compared to Mode B. This could be understood that, for Mode A fracture, the crack bridging, due to the fibers' bridging (see Fig 5c), alongside its resultant fibers' debonding is the most significant toughening mechanism which is responsible for the exhibited strength asymmetry. As demonstrated in Fig. 5a, separation of a matrix crack which is bridged by uniaxially aligned fibers requires sliding of the matrix over the fibers [26]. The sliding however is restricted by frictional forces that consequently lead to a reduction in the crack surface displacement, which is equivalent to applying a closure stress on the crack surfaces. Hence, owing to crack bridging, higher load needs to be applied to initiate the crack. This reduction in stress at the crack tip can be expressed as [26]:

$$K_{tip} = K_a - K_s \tag{6}$$

where K_{tip} is the local stress intensity factor at the crack tip, K_a is the applied stress intensity factor and K_s is the shielding stress intensity factor.

It is moreover remarkable to note that the influence of fibers on crack bridging amplifies with a decrease in the distance of fibers from the crack tip; in a way that if during crack propagation the crack encounters a second row of fibers, the crack growth resistance would be enhanced further. However, in the case of very

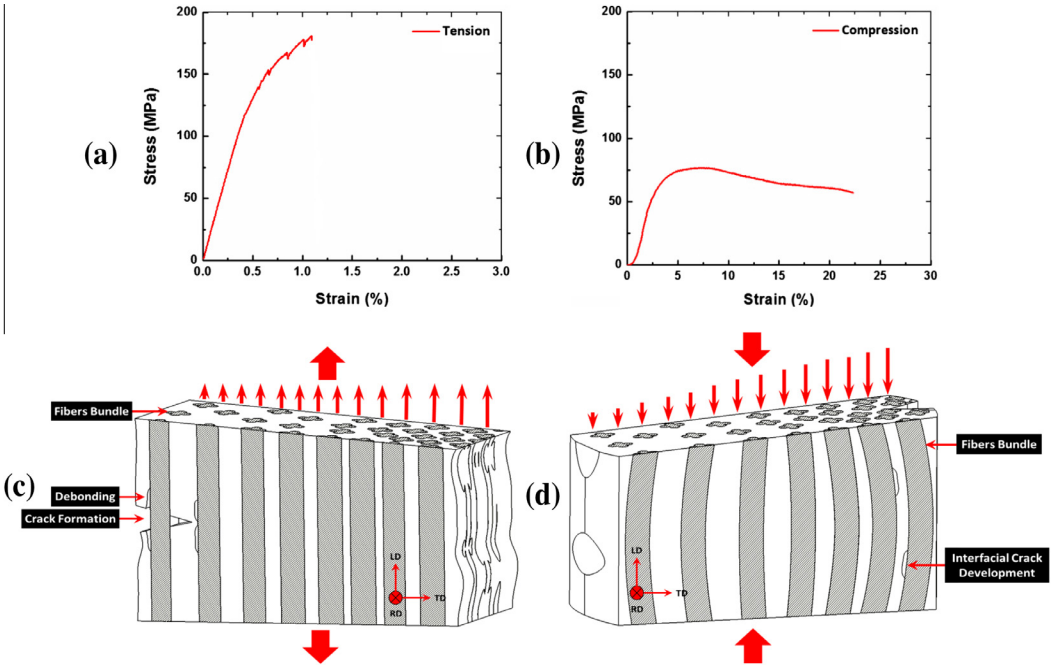

Fig. 8. Tension–compression asymmetry: (a and b) stress–strain curves along with (c and d) schematic representations of deformation behavior of bamboo culm in the case of tensile and compressive loading, respectively (The schematic demonstration of the deformed specimens and the arrows across the samples' cross section indicate the evolution of strain heterogeneity and distribution of the load within the samples, in the case of each loading mode, respectively).

large fiber volume fraction, the occurrence of crack bridging alongside its resultant fibers' debonding diminishes owing to reduced matrix spacing [11,25]. Accordingly, the layers with very large volume fraction of fibers result in very low extent of crack bridging and fibers' debonding in Mode B, because "delamination" occurred more often (see Fig. 5e), which considerably reduce the flexural strength. This could be also inferred by a comparison among the exhibited serrations in the stress–strain curves during each loading mode (see Fig. 3). The presence of more serrations in the stress–strain curves of bamboo strips subjected to Mode B rather than Mode A is an evidence of more delamination occurrence in the course of Mode B compared to Mode A.

For the higher toughness in Mode A than that in Mode B, it can be largely attributed to the role of foam-like parenchyma cells on accommodating the large deformation by getting squeezed, during elastic bending, resulted in much larger flexural ductility (flexibility) for Mode B than Mode A. More importantly, by inducing "tortuous crack propagation" [14] along their interfacial areas during fracture failure, parenchyma cells could further enhance the bamboo's superior flexural toughness—although it is a general mechanism for enhancing the fracture toughness [14], the much larger interface areas created by delamination processes in Mode B considerably increased the interfacial fracture occurrences (Fig. 6a) between delaminated parenchyma cells (as evidenced by the intact parenchyma cells in Fig. 6b), making the "tortuous crack propagation" a dominating factor for differentiating the toughness during Mode B "fracture failure" stage. So even the overall strengths of Mode B were lower than that of Mode A, its fracture toughness could be still higher than that of Mode A.

4.3. Tension–compression asymmetry

From the results and above discussions, it has been shown that the exhibited asymmetry in the "elastic bending" depends more on the deformation mechanisms from the top layer of bamboo strips (loading side), whereas the asymmetry during "fracture failure" seemed to be more related with the characteristics from the bottom layer (as fracture always occurred from the bottom layer). Considering standard three-point bending model (Fig. 2) where the top layer should be under compression while the bottom layer should under tension, we additionally performed tensile and compressive experiments along the longitudinal direction (fibers' direction) of the bamboo culm specimen, to assess the difference in accommodating large deformation and its possible relation with the origin of the flexural asymmetry. Interestingly, we again observed asymmetric responses from the uniaxial tension and compression tests (see Fig. 8). As displayed in Fig. 8a–b, bamboo culm demonstrated larger strength but smaller ductility in the course of tension than that of compression. The developed strain heterogeneity, as shown in Fig. 8c–d was mostly from the gradient distribution of load due to bamboo's FG structure. The disclosed asymmetry in strength could be basically justified by the existence of crack bridging and deflection mechanisms in the case of tension, whereas the demonstrated asymmetry in failure strain (ductility) could be mainly attributed to the squeezing of the parenchyma cells during the compression, which were both very similar to that of flexural bending. However, unlike in bending tests fracture mostly occurs in tension area, we discovered very different fracture mechanism in severe compressed specimen—the formation of shear band (see Fig. 9a), due to the fibers' buckling (see Fig. 9b), as well as crack initiated and nucleated when shear band met the interface of fiber bundle and parenchyma ground (as displayed in Fig. 9c). Lastly, the significant larger compression ductility (up to ~15–20%) than that in tension and bending (a few percentages) confirmed that bamboo materials can indeed sustain much larger deformation in compression than in tension, resulted in the often occurrences of fracture failure at the bottom layer of the bent bamboo strips.

5. Conclusions

In summary, bamboo material's remarkable flexural properties are stemmed out from the concurrent graded distribution of

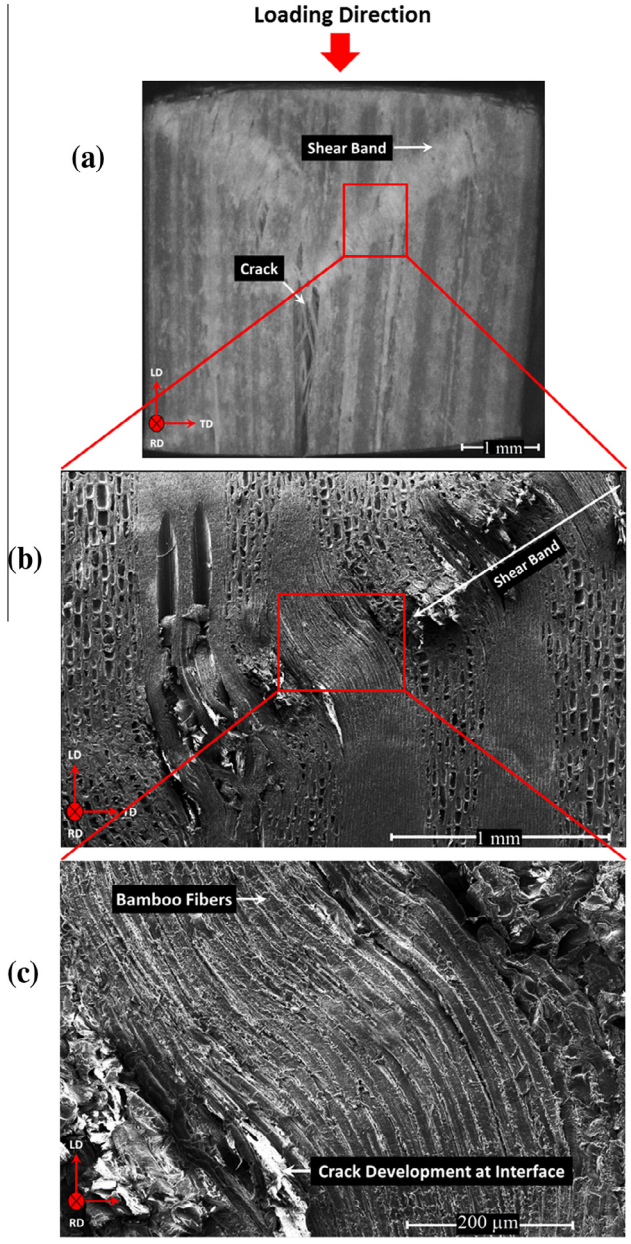

Fig. 9. Shear band formation in the compressively deformed specimen: (a) optical and (b and c) SEM micrographs representing the formation of shear bands in bamboo culm, subjected to longitudinal compression; (c) represents the fibers buckling as well as crack formation at the matrix-fibers interfaces.

tougher constituent (mainly fibers), along with weaker constituent (such as parenchyma cells). Induced by their FG hierarchical structure, bamboo strips demonstrate significant asymmetric flexural behavior and distinctly different underlying mechanisms when loaded from the inner and outer sides during the elastic bending and fracture failure stages. Similar asymmetric behavior has been also disclosed in uniaxial loading of bamboo culm specimen, indicating the important role of the microstructural features in determining the macroscopic asymmetry in bamboo's mechanical behavior. The insights obtained from this systematic experimental study, along with the numerical model, shall be useful for the biomimicking purposes in fabrication and processing of advanced structural materials with desired flexural behavior.

Acknowledgments

The authors gratefully acknowledge the financial support from City University of Hong Kong under the Grants # 7003021, # 9610288 and # 9667098, as well as the CityU International Transition Team Scheme (ITT-GTA) postdoctoral fellowship.

Appendix A. Figures with essential color discrimination

Certain figures in this article, particularly Figs. 1–9, are difficult to interpret in black and white. The full color images can be found in the on-line version, at http://dx.doi.org/10.1016/j.actbio.2015.01.038.

References

[1] Wegst UG, Bai H, Saiz E, Tomsia AP, Ritchie RO. Bioinspired structural materials. Nat mater 2014.
[2] Dixon PG, Gibson LJ. The structure and mechanics of Moso bamboo material. J R Soc Interface 2014;11:20140321.
[3] Gershon AL, Bruck HA, Xu S, Sutton MA, Tiwari V. Multiscale mechanical and structural characterizations of Palmetto wood for bio-inspired hierarchically structured polymer composites. Mater Sci Eng, C 2010;30:235–44.
[4] Silva ECN, Walters MC, Paulino GH. Modeling bamboo as a functionally graded material: lessons for the analysis of affordable materials. J Mater Sci 2006;41:6991–7004.
[5] Low IM, Che ZY, Latella BA. Mapping the structure, composition and mechanical properties of bamboo. J Mater Res 2006;21:1969–76.
[6] Suresh S, Mortensen A. Fundamentals of functionally graded materials. The Institute of Materials, 1998.
[7] Huang D, Zhou A, Li H, Su Y, Chen G. Experimental study on the tensile properties of bamboo related to its distribution of vascular bundles. 2012. p. 112–7.
[8] Obataya E, Kitin P, Yamauchi H. Bending characteristics of bamboo (*Phyllostachys pubescens*) with respect to its fiber-foam composite structure. Wood Sci Technol 2007;41:385–400.
[9] Shao ZP, Fang CH, Huang SX, Tian GL. Tensile properties of Moso bamboo (*Phyllostachys pubescens*) and its components with respect to its fiber-reinforced composite structure. Wood Sci Technol 2010;44:655–66.
[10] Shao Z-P, Fang C-H, Tian G-L. Mode I, interlaminar fracture property of moso bamboo (*Phyllostachys pubescens*). Wood Sci Technol 2009;43:527–36.
[11] Tan T, Rahbar N, Allameh SM, Kwofie S, Dissmore D, Ghavami K, et al. Mechanical properties of functionally graded hierarchical bamboo structures. Acta Biomater 2011;7:3796–803.
[12] Wegst UG. Bamboo and wood in musical instruments. Mater Res 2008;38:323.
[13] Yu H, Fei B, Ren H, Jiang Z, Liu X. Variation in tensile properties and relationship between tensile properties and air-dried density for moso bamboo. Front For China 2008;3:127–30.
[14] Habibi MK, Lu Y. Crack propagation in bamboo's hierarchical cellular structure. Sci Rep 2014;4.
[15] Flores M, Fernández-Francos X, Ferrando F, Ramis X, Serra À. Efficient impact resistance improvement of epoxy/anhydride thermosets by adding hyperbranched polyesters partially modified with undecenoyl chains. Polymer 2012;53:5232–41.
[16] Bobji MS, Biswas SK. Estimation of hardness by nanoindentation of rough surfaces. J Mater Res 1998;13:3227–33.
[17] Baker SP. Between nanoindentation and scanning force microscopy: measuring mechanical properties in the nanometer regime. Thin Solid Films 1997;308–309:289–96.
[18] Oliver WC, Pharr GM. Measurement of hardness and elastic modulus by instrumented indentation: advances in understanding and refinements to methodology. J Mater Res 2004;19:3–20.
[19] Wang X, Ren H, Zhang B, Fei B, Burgert I. Cell wall structure and formation of maturing fibres of moso bamboo (*Phyllostachys pubescens*) increase buckling resistance. J R Soc Interface 2011 (rsif20110462).
[20] Yu Y, Tian G, Wang H, Fei B, Wang G. Mechanical characterization of single bamboo fibers with nanoindentation and microtensile technique. Holzforschung 2011;65:113–9.
[21] Villalobos Camargo G. A statistical model of fracture due to drying in bamboo guadua angustifolia: Universidad Nacional de Colombia; 2012.
[22] Amada S, Untao S. Fracture properties of bamboo. Compos B Eng 2001;32:451–9.
[23] Amada S, Ichikawa Y, Munekata T, Nagase Y, Shimizu H. Fiber texture and mechanical graded structure of bamboo. Compos B Eng 1997;28:13–20.
[24] Wakashima K, Hirano T, Niino M. Space applications of advanced structural materials. ESA SP 1990;303:97.
[25] Ostertag C. Experimental evidence of crack tip shielding mechanisms in quasi-brittle materials. J Mater Sci 1997;32:4011–7.